

# Sonocatalytic degradation of 2-Mercaptobenzothiazole (MBT) in aqueous solution by a green catalyst Maghnite-H<sup>+</sup>

Kawther Nesrine Benkhemkhem , Sarra Bourahla\* , Hanane Belayachi ,  
Fadela Nemchi , Mostefa Belhakem 

*Laboratoire de Structure, Elaboration et Application des Matériaux Moléculaires (SEA2M), Faculté des Sciences Exactes et de l'Informatique (FSEI), Université Abdelhamid Benbadis, Mostaganem, Algeria.*

\*Corresponding author: [sarra.bourahla@univ-mosta.dz](mailto:sarra.bourahla@univ-mosta.dz)

## Original Research

## Abstract:

Received:  
14 December 2023  
Revised:  
26 January 2024  
Accepted:  
03 April 2024  
Published online:  
17 May 2024

© The Author(s) 2024

The sonocatalytic activity of the particles of the green Maghnite-H<sup>+</sup> sonocatalyst was tested by the degradation of 2-Mercaptobenzothiazole (MBT) under ultrasonic irradiation was performed in an ultrasonic bath with a frequency of 40 kHz, and an ultrasonic power of 120 W for 120 min at room temperature followed by UV-visible analysis. This study was accompanied by the application of a commercial catalyst approved in the literature, TiO<sub>2</sub>-anatase. The catalysts used were characterized by X-ray diffraction (XRD), Fourier transform infrared spectroscopy (FT-IR), Brunauer–Emmett–Teller (BET), and the band gap energy of Maghnite-H<sup>+</sup> was determined by the Tauc method. Different experimental conditions, such as the dose of the catalyst, the initial concentration of MBT, and the addition of H<sub>2</sub>O<sub>2</sub>, were studied to determine their effects on sonocatalytic degradation. At a concentration of [MBT] = 10 mg.L<sup>-1</sup>, the degradation rates of MBT after 120 min of sonocatalysis are 94.29% for Maghnite-H<sup>+</sup> and 40.22% for TiO<sub>2</sub>-anatase. The effect of the concentration of MBT is proportional to the rate of degradation. The addition of H<sub>2</sub>O<sub>2</sub> (0.5 mol. L<sup>-1</sup>) improved the efficiency of the degradation to 97% for the Maghnite-H<sup>+</sup> and 87.85% for the TiO<sub>2</sub>-anatase. For an initial MBT concentration of 10 mg.L<sup>-1</sup>, the total organic carbon (TOC) measurement revealed that after 120 minutes, 82.79% and 28.54% mineralization was observed for US/Maghnite-H<sup>+</sup> and US/TiO<sub>2</sub> systems, respectively.

**Keywords:** Sonocatalytic degradation; Maghnite-H<sup>+</sup>; TiO<sub>2</sub>-anatase; 2-Mercaptobenzothiazole; UV-visible analysis

## 1. Introduction

With the rapid development of the chemical industry, environmental pollution by organic compounds remains a major concern, as the presence of these compounds and their increased concentration led to toxicity risks for aquatic organisms and humans [1–4]. Mercaptans, as a class of chemicals, have been widely applied in many areas [5, 6]. 2-Mercaptobenzothiazole (MBT) is a mercaptan and an important chemical additive involved in the synthesis of industrial products. It is widely used as a vulcanization accelerator in the rubber industry and also serves as a

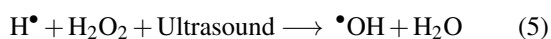
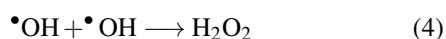
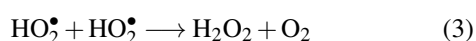
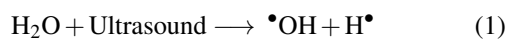
sensitive reagent for testing herbicides and cephalosporin synthesis intermediates [7]. Moreover, it should be noted that inhaling low concentrations of MBT causes nausea and headaches, as MBT has certain toxicity and is difficult to eliminate [8].

Over the last few decades, the removal of pollutants from the environment has been researched as an economically viable procedure. This is achieved by reducing contaminants through the use of semiconductors, sonocatalysts, and photocatalysts with advanced oxidation processes. Advanced oxidation processes (AOPs) are particularly efficient at degrading complex pollutants in water, outperforming

conventional methods in the treatment of resistant and toxic compounds. These processes rely on highly reactive species, enabling more advanced degradation than standard treatments [9].

However, this research concentrated on an advanced oxidation technique for degrading MBT in industrial effluent. Among various advanced oxidation processes, ultrasonic degradation is a promising technique which has been broadly used over the last two decades [10–12], proven due to its simple equipment, high efficiency, stable operation, safety, and no secondary pollution [13, 14].

The sonocatalytic degradation of organic pollutants can be described as an ultrasonic cavitation effect in an aqueous medium [15]. This leads to sonoluminescence, to the hot spot which induces the dissociation of the water molecule into a hydroxyl radical ( $\bullet\text{OH}$ ) (Eq. 1-5) which is a powerful oxidant, responsible for the degradation and mineralization of organic compounds [16–18].



The sonocatalytic degradation of wastewater can be used in the presence of a sonocatalyst. In this study, we used a chemically modified clay, Maghnite- $\text{H}^+$ , as a green sonocatalyst.

The purpose of this research was to develop products that reduce the use of hazardous substances in line with the concept of green chemistry [19–21]. In addition, the availability of bentonite deposits in Algeria, particularly the Maghnia quarry (Hammam Boughrara), with reserves estimated at 1 million tonnes [22, 23].

Based on the literature, few works use Maghnite- $\text{H}^+$  as a green sonocatalyst for the degradation of organic pollutants. However, the application of Maghnite- $\text{H}^+$  particles for the sonocatalytic degradation process has not been considered so far.

In order to prove the catalytic efficiency of the decomposition of MBT using a natural source sonocatalyst: Maghnite- $\text{H}^+$ , a comparative study between the latter and  $\text{TiO}_2$ -anatase was carried out.

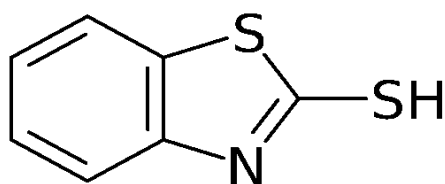


**Figure 1.** Topological structure of 2-Mercaptobenzothiazole.

## 2. Experimental

### 2.1 Materials

The nanoparticles of  $\text{TiO}_2$ -anatase (99.7% purity) of size 25 nm and specific surface of  $220 \text{ m}^2 \cdot \text{g}^{-1}$ , supplied by Sigma-Aldrich, were used. 2-Mercaptobenzothiazole was provided by Sigma-Aldrich, CHEMIE GmbH, a Product of China, with 97% purity. Aqueous solutions of MBT at various concentrations were prepared in a basic medium [24]. Other chemicals used are sulfuric acid (98%, Biochem Chemopharma) and hydrogen peroxide (34.5–36.5%, Sigma-Aldrich). Table 1 shows some characteristics of MBT. Figure 1 shows the chemical structure of the pesticide.

### 2.2 Preparation of Maghnite- $\text{H}^+$

The montmorillonite was collected in Maghnia, western Algeria. Maghnite- $\text{H}^+$  was prepared as follows: 30 g of raw Maghnite was mixed with 120 ml of distilled water at room temperature. The suspension obtained is left under stirring for 30 min, after which 100 ml of a solution of  $\text{H}_2\text{SO}_4$  (0.23 M) will be added. Stirring is maintained for 48 h. After filtration and washing, the activated Maghnite was dried at  $105^\circ\text{C}$  for 24 hours. Finally, grind, sieve, and store away from air and humidity [25].

### 2.3 Samples characterizations

FTIR spectra were determined using a Shimadzu IR-Prestige 21 spectrometer in the wavelength range of  $400\text{--}4000 \text{ cm}^{-1}$  and a resolution of  $4 \text{ cm}^{-1}$ . The pellets were made from a mixture of sample and potassium bromide under pressure. Characterization by X-ray diffraction of the samples was carried out on a Miniflex-600 diffractometer in Tokyo, Japan. Textural characteristics were studied using  $\text{N}_2$  adsorption-desorption analysis at 77 K on an ASAP 2020 Micrometrics instrument. The UV-vis DRS of the samples were recorded using a Shimadzu UV-2550 (Japan) spectrophotometer. A Shimadzu UV-1280 series spectrophotometer equipped with quartz cells (Optical length=1.0 cm) was used to detect the UV absorption of each sample. The scan range was 190~600 nm. For the determination of the band gap of Maghnite- $\text{H}^+$ , analysis by a UV-visible solid spectrophotometer was performed. The mineralization was measured through the determination of the total organic carbon concentration (TOC) via Analytik-Jena multi-N/C, the 2100S.

### 2.4 Sonocatalytic degradation

The sonocatalytic activity of the materials was studied for MBT degradation from basic aqueous solution [24] using an ultrasonic bath with a frequency of 40 kHz, an ultrasonic

**Table 1.** Some characteristics of 2-Mercaptobenzothiazole.

chemical formula	$\text{C}_7\text{H}_5\text{NS}_2$
molecular weight ( $\text{g} \cdot \text{mol}^{-1}$ )	167.25
$\lambda_{\text{max}}$	320 nm
color	yellow
pH	6.3

power of 120 W ("Ultrasonic-HD" baths with heating, digital electronic temperature, and time control, J.P SELECTA Spain), the machine's energy consumption is 195 W. The experimental apparatus was covered to prevent photocatalysis. In each experiment, a specific amount of catalyst was added to 0.025 L of MBT aqueous solution in a beaker. The resulting solution was magnetically stirred for 60 min to make a good dispersion of Maghnite-H<sup>+</sup> particles into the MBT with the aim of providing a larger contact surface between the catalyst and the pollutant and then submitted to ultrasonic irradiation. The following degradation experiments aimed to determine the effect of mass, the effect of initial concentration, the effect of adding H<sub>2</sub>O<sub>2</sub>, and the spectral evolution of degradation after 120 min of treatment. All degradation experiments were performed in 0.025 L glass vials (with caps) in the dark at a constant temperature of 25 °C at natural pH (Fig. 2); the temperature was controlled during the sonocatalysis system using the temperature control button on the machine. Aliquots were taken at regular intervals and examined with a UV-Vis spectrophotometer with a maximum MBT wavelength of 320 nm. The degradation efficiency (DE%) was determined using the following equation [26] based on the change in MBT concentration before and after treatment:

$$DE(\%) = \frac{C_0 - C_t}{C_0} \times 100\% \quad (6)$$

where  $C_0$  and  $C_t$  are the dye concentrations at reaction time  $t=0$  and  $t$ , respectively. Using a Shimadzu TOC analyzer, the total organic carbon concentration (TOC) was determined in order to quantify the mineralization. The extent of mineralization for the MBT solution was calculated by evaluating the percentage of Total Organic Carbon removed, using the formula provided in equation [27]:

$$\%TOC_{\text{removal}} = \frac{(TOC_0 - TOC_t)}{TOC_0} \times 100\% \quad (7)$$

The values  $TOC_t$  and  $TOC_0$  represent the TOC value at time  $t$  and the initial TOC value, respectively.

### 3. Results and discussion

#### 3.1 Characterization of Maghnite-H<sup>+</sup> and TiO<sub>2</sub>-anatase

FTIR spectroscopy is an important tool that allows the identification of functional groups contained in samples. Maghnite-H<sup>+</sup> and TiO<sub>2</sub>-anatase spectra are shown in Fig. 3. For Maghnite-H<sup>+</sup>, the bands located at 3436 and 3630 cm<sup>-1</sup> are characteristic of the stretching vibrations of the OH bond of the interlayer water and the stretching vibrations of the OH groups of the octahedral layer, respectively [28]. The adsorption band at 1656 cm<sup>-1</sup> is attributed to the angular deformation OH of water, and the intense band at 1033 cm<sup>-1</sup> corresponds to the stretching vibration of the Si-O bond [29]. The bands at 787, 525, and 467 cm<sup>-1</sup> are attributed to the deformation vibrations of the Si-O-M bond (M denotes the metals Al, Mg, Si, and Fe located in octahedral position) [30].

The FTIR spectrum of TiO<sub>2</sub>-anatase contains two bands at 3411 and 1633 cm<sup>-1</sup>, which are attributed, respectively, to elongation vibrations and angular deformation of the OH bond (Ti-OH) resulting from the presence of water traces. 3218 cm<sup>-1</sup> is a characteristic shoulder of the stretching vibration of adsorbed water molecules on Ti (Ti-OH<sub>2</sub>) [31, 32]. The intense band in the 450-750 cm<sup>-1</sup> range is due to the different vibrational modes of the Ti-O-Ti bond [32, 33].

In previous investigations, the structure and composition of Maghnite-H<sup>+</sup> were described [34–36]. The basic structure of Maghnite-H<sup>+</sup> is similar to that of montmorillonite, which belongs to the smectite family. Smectites are characterized by a layered structure, with a central layer of aluminum or magnesium octahedra surrounded by two tetrahedral layers of silica [37]. What distinguishes Maghnite-H<sup>+</sup> is the presence of hydrogen ions (protons) in the cation exchange sites between the silicate layers, as illustrated in Fig. 4. TiO<sub>2</sub>-anatase has a tetragonal structure and also has a low energy crystal plane, so it can show as a truncated octahedron [38].

Fig. 5 shows the X-ray diffraction pattern of the sulfuric acid-treated Maghnite. The diffractogram of the ac-

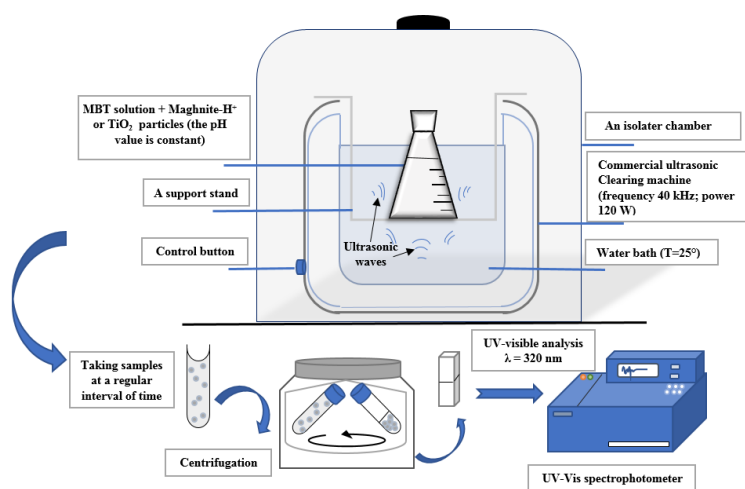


**Figure 2.** Schematic illustration of the sonocatalytic degradation process of 2-Mercaptobenzothiazole by Maghnite-H<sup>+</sup> and TiO<sub>2</sub>.

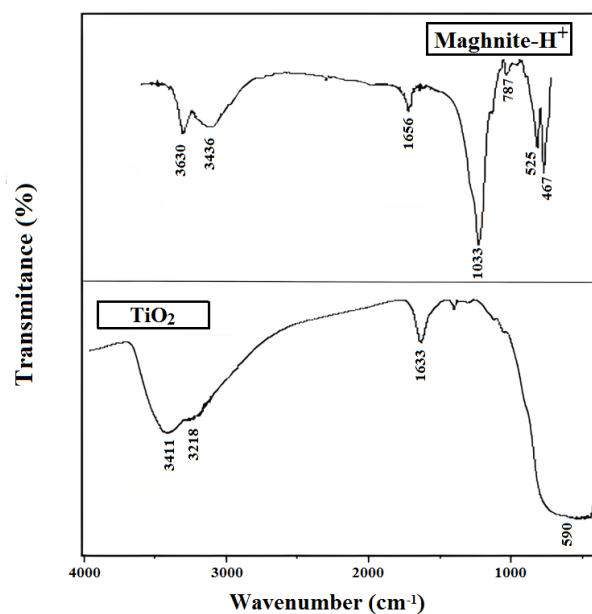


Figure 3. FT-IR transmission spectra of Maghnite-H<sup>+</sup> and TiO<sub>2</sub>-anatase.

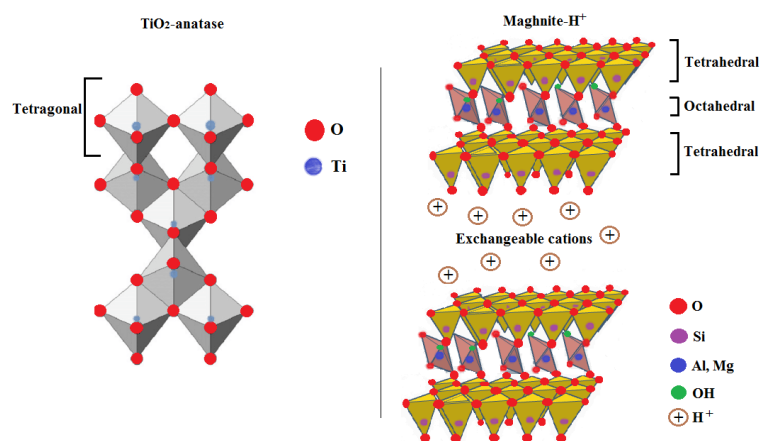


Figure 4. Crystallographic structure of Maghnite-H<sup>+</sup> and TiO<sub>2</sub>-anatase.

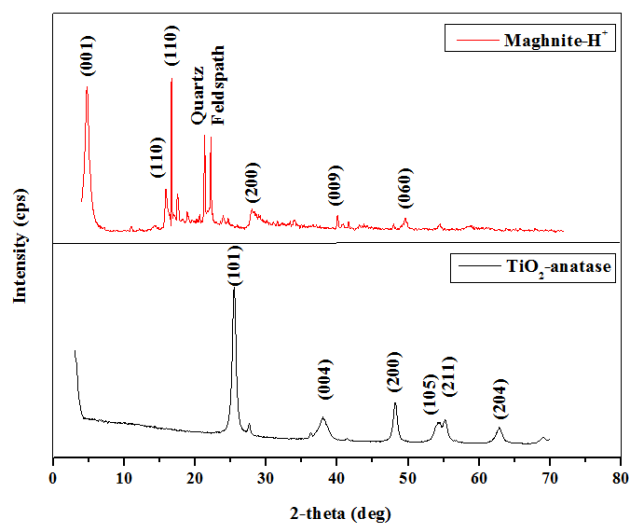


Figure 5. XRD patterns of Maghnite-H<sup>+</sup> and TiO<sub>2</sub>-anatase.

tivated Maghnite shows a series of peaks characteristic of the montmorillonite phase, which correspond to lattice distances 5.95° (001), 19.85° (110), 20.83° (110), 35.01° (200), 50.07° (009) and 61.73° (060) (Table 2), the acid treatment of Maghnite eliminates all traces of calcite [39, 40]. In the same diffractogram, Maghnite-H<sup>+</sup> contains impurities in the form of Quartz (26.65°) and Feldspath (27.73°) [41].

XRD analysis of TiO<sub>2</sub>-anatase (Fig. 5) shows the presence of an anatase phase with broad peaks appearing at 25.56°, 38.20°, 48.17°, 54.28°, 55.26°, and 63.00°, which corresponded to the crystal planes (101), (004), (200), (105), (211), and (204), respectively [42, 43].

The crystallites size (D) of the Maghnite-H<sup>+</sup> and TiO<sub>2</sub>-anatase was respectively calculated from the widths at half maximum height using the Debye-Scherrer equation [44]:

$$D = \frac{K\lambda}{\beta \cos \theta} \quad (8)$$

where  $\lambda$  is the X-ray wavelength of the incident beam (1.540593Å),  $\theta$  is the Bragg angle, the FWHM is the strain, and  $K$  is a constant, approximately equal to 0.9, related to the domain shape. The structural parameters for Maghnite-H<sup>+</sup> and TiO<sub>2</sub>-anatase are represented in Table 2.

Fig. 6 shows the adsorption-desorption isotherms of N<sub>2</sub> (77 K) and the pore size distribution of the Maghnite-H<sup>+</sup>. According to the IUPAC classification, the isotherm is type II with H4 hysteresis loop; this explains that the Maghnite-H<sup>+</sup> contains mostly mesopores with only a small contribution of micropores (Table 3) [45]. The BET surface (SBET) of the Maghnite-H<sup>+</sup> is 58.88 m<sup>2</sup>.g<sup>-1</sup>, and the pore size distribution indicates the presence of mesoporous structures with an average pore diameter of 5.6 nm (Table 3), which were respectively similar to other reported Maghnite-H<sup>+</sup> [46, 47].

The absorbance spectrum of Maghnite-H<sup>+</sup> is shown in Fig. 7. The spectrum shows a region of strong absorption corresponding to the fundamental absorption, after which the spectrum begins to decrease. This variation corresponds to the band gap [48]. The band gap energy of Maghnite-H<sup>+</sup> was determined through the Tauc method according to the following equation [49]:

$$(\alpha h\nu)^2 = A(h\nu - E_g) \quad (9)$$

where  $\alpha$  is the absorption coefficient,  $h\nu$  is the photon energy (eV),  $A$  is a constant, and  $E_g$  is the band gap. The band gap energy was obtained by extrapolating the linear portion of the  $(\alpha h\nu)^2$  curve versus  $h\nu$  (Fig. 7). From this, the band gap value of Maghnite-H<sup>+</sup> is 3.51 eV. According to the literature, the band gap of TiO<sub>2</sub>-anatase is ~3.20 eV [50].

## 3.2 Degradation study

### 3.2.1 Dose effect

Figure 8 shows the sonocatalytic degradation of MBT for the samples studied (Maghnite-H<sup>+</sup> and TiO<sub>2</sub>-anatase) at variable doses ranging from 0.4 to 4 g.L<sup>-1</sup> versus time (min) under irradiation of 40 kHz, [MBT] = 100 mg. L<sup>-1</sup> and temperature of 25°C, in dark conditions. The efficiency of sonocatalysis increases with increasing catalyst concentration. The optimal dose of Maghnite-H<sup>+</sup> particles is obtained at 3 g.L<sup>-1</sup>. For TiO<sub>2</sub>-anatase, efficiency increases up to a catalyst concentration of 1.2 g.L<sup>-1</sup>, but decreases above this dose. The percentages of MBT degradation after 120 min of sonocatalysis is 65.17% and 15.98% for Maghnite-H<sup>+</sup> and TiO<sub>2</sub>-anatase, respectively. In general, appropriately increasing the catalyst dosage increases the active sites of the sonocatalyst and increases pollutant removal. However, the excessive addition of catalyst reduces the number of active sites due to proximity and aggregation between active sites [57].

### 3.2.2 Effect of initial MBT concentration on the degradation of MBT

The effect of the initial concentration of MBT on the efficiency of sonolysis using catalysts (Maghnite-H<sup>+</sup> and TiO<sub>2</sub>-anatase) was performed at T= 25 °C, [Maghnite-H<sup>+</sup>]=3 g.L<sup>-1</sup> and [TiO<sub>2</sub>-anatase]=1.2 g.L<sup>-1</sup> is presented in Fig. 9. Increasing the initial concentration of MBT reduced the degradation from 94.29% to 37.40% for a time of 120 min in the presence of Maghnite-H<sup>+</sup> and from 40.22% to 7.88% for TiO<sub>2</sub>-anatase, as has been observed previously with certain organic dyes [58, 59]. This behavior can be explained by the fact that higher concentrations of intermediates are formed with increasing MBT initial concentration. Assuming that most reactions take place at the bubble-liquid interface, with

**Table 2.** The structural parameters for Maghnite-H<sup>+</sup> and TiO<sub>2</sub>-anatase.

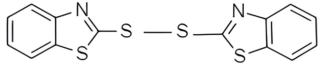
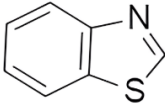
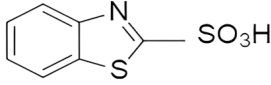
	2θ (deg)	Hkl	FWHM (deg)	D (nm)
Maghnite-H <sup>+</sup>	5.95	(001)	1.25	6.363984584
	19.85	(110)	1.10	7.331779868
	20.83	(110)	0.90	8.974822
	35.01	(200)	1.90	4.384219026
	50.07	(009)	0.40	21.9200459
	61.73	(060)	0.72	12.85410989
TiO <sub>2</sub> -anatase	25.56	(101)	0.6272	12.98798591
	38.20	(004)	1.12	7.506319304
	48.17	(200)	0.8201	10.61069459
	54.28	(105)	1.1875	7.517633877
	55.60	(211)	0.7824	11.47854652
	63.00	(204)	0.875	10.64828008



**Table 3.** Production of **4e** via various solvents<sup>a</sup>.

	$S_{BET}$ ( $m^2 \cdot g^{-1}$ )	porosity properties			
		$V_t$ ( $cm^3 \cdot g^{-1}$ )	$V_{micro}$ ( $cm^3 \cdot g^{-1}$ )	$V_{meso}$ ( $cm^3 \cdot g^{-1}$ )	$d_p$ (nm)
Maghnite-H <sup>+</sup>	58.88	0.057	0.011	0.046	5.6

**Table 4.** The proposed structure at each wavelength as a function of time [7, 51].

time (min)	wavenumber (nm)	proposed structure
15	226 277	
30 60	216 252	
90 120	263	

**Table 5.** Comparative table of different catalysts used in the sonocatalytic degradation process.

catalyst	pollutant	concentration pollutant	catalyst dosage	ultrasonic power/frequency	reaction time	degradation efficiency	reference
Bismuth tungstate Bi <sub>2</sub> WO <sub>6</sub>	Methyl Orange MO	10 mg. L <sup>-1</sup>	1.0 g. L <sup>-1</sup>	400 W/ 40kHz	30 min	80%	[52]
Zinc Oxide on Montmorillonite (MMT-ZnO)	Naproxen	10 mg. L <sup>-1</sup>	0.5 g. L <sup>-1</sup>	650 W/60 kHz	120 min	73.60%	[53]
Porous trigonal TiO <sub>2</sub> nanoflakes (p-TiO <sub>2</sub> )	Rhodamine B (RhB)	5 mg. L <sup>-1</sup>	0.5 g. L <sup>-1</sup>	80 W/40 kHz	180 min	81%	[54]
Maghnite-H <sup>+</sup>	2-Mercaptobenzothiazole	10 mg. L <sup>-1</sup>	3 g. L <sup>-1</sup>	120 W/40 kHz	120 min	94.29%	this work
TiO <sub>2</sub> -anatase	2-Mercaptobenzothiazole	10 mg. L <sup>-1</sup>	1.2 g. L <sup>-1</sup>	120 W/40 kHz	120 min	40.22%	this work
CoFe <sub>2</sub> O <sub>4</sub> /mpgC <sub>3</sub> N <sub>4</sub>	Methylene blue	8 mg. L <sup>-1</sup>	0.25 g. L <sup>-1</sup>	665 W/40 kHz	45 min	92.81%	[55]
Tungsten disulfide (WS <sub>2</sub> )	Basic violet 10	10 mg. L <sup>-1</sup>	1.0 g. L <sup>-1</sup>	400 W	150 min	94.01%	[56]

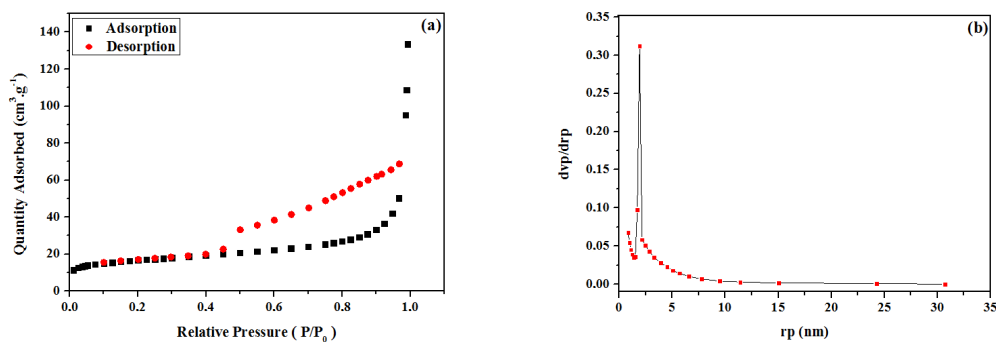


Figure 6. (a) N<sub>2</sub> adsorption-desorption isotherm at 77 K and (b) Pore size distribution of Maghnite-H<sup>+</sup>.

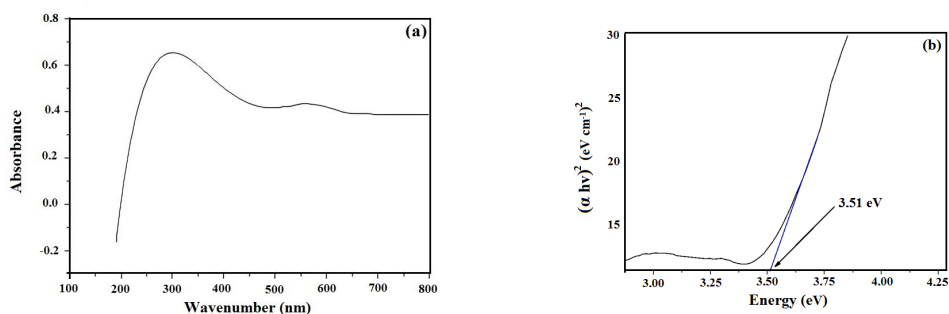


Figure 7. UV-visible spectrum (a) calculated band gap energies by the Tauc method and (b) for Maghnite-H<sup>+</sup>.

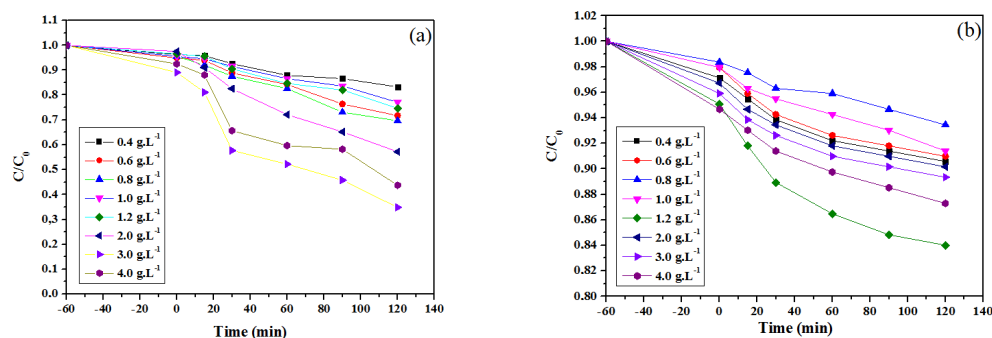


Figure 8. (a) Effect of the dose of Maghnite-H<sup>+</sup> and (b) TiO<sub>2</sub>-anatase on the sonocatalytic degradation of MBT. F= 40 kHz, [MBT] = 100 mg. L<sup>-1</sup>, T = 25 °C.

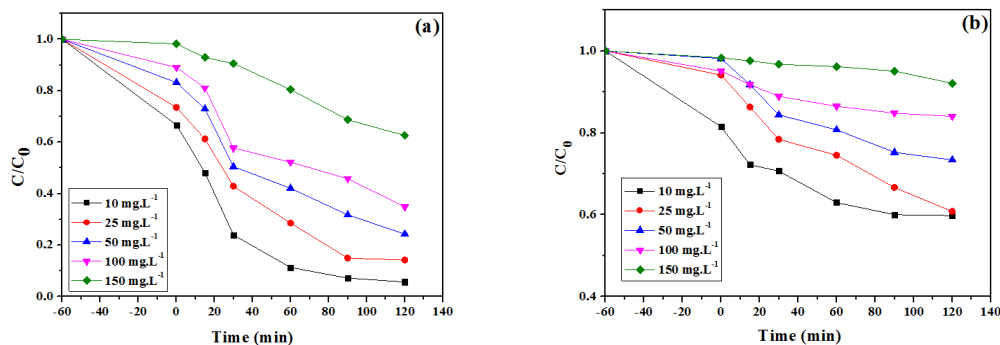


Figure 9. (a) Effect of MBT concentration on its sonocatalytic degradation by Maghnite-H<sup>+</sup> and (b) TiO<sub>2</sub>-anatase F= 40 kHz, [Maghnite-H<sup>+</sup>] = 3 g.L<sup>-1</sup>, [TiO<sub>2</sub>-anatase] = 1.2 g.L<sup>-1</sup>, T = 25 °C.

increasing initial concentration of MBT and corresponding intermediates, MBT degradation was limited by the available interfacial area [60]. However, Maghnite-H<sup>+</sup> favors the degradation of MBT, probably by the production of reactive species under irradiation.

### 3.2.3 Effect of H<sub>2</sub>O<sub>2</sub> concentration

The percentage of sonocatalytic degradation of MBT by Maghnite-H<sup>+</sup> and TiO<sub>2</sub>-anatase at different H<sub>2</sub>O<sub>2</sub> concentrations (0–0.75 mol.L<sup>-1</sup>) was investigated, and the results are shown in Fig. 10. The histogram shows that the degradation of MBT is accelerated by increasing the concentrations of hydrogen peroxide with a degradation rate of 97% and 87.85% for the system US-Maghnite-H<sup>+</sup>-H<sub>2</sub>O<sub>2</sub> and US-TiO<sub>2</sub>-anatase-H<sub>2</sub>O<sub>2</sub>, respectively. The hydroxyl radicals are generated with increasing concentration of H<sub>2</sub>O<sub>2</sub> but remain constant when the concentration increases further. Nevertheless, it has been mentioned in the literature that an excessive increase in the concentration of H<sub>2</sub>O<sub>2</sub> induces a self-inhibitory effect of hydroxyl radicals [61]. However, increasing the amount of H<sub>2</sub>O<sub>2</sub> by 0.5 and 0.75 mol.L<sup>-1</sup> did not lead to greater degradation but acted as a hydroxyl radical scavenger and the hole scavenger (h<sup>+</sup>) [62, 63]. Thus, 0.25 mol.L<sup>-1</sup> was chosen as the optimal amount of H<sub>2</sub>O<sub>2</sub> for MBT degradation.

### 3.3 Study of UV-visible absorption spectra and reaction mechanism

Figure 11 shows the UV-Vis spectra of MBT in solution irradiated by ultrasound for 120 min in the presence of Maghnite-H<sup>+</sup> particles. The UV-vis spectrum of the MBT (Fig. 11) contains three absorption peaks (203, 230, and 315 nm) and one shoulder at 253 nm. Figure 8 shows a sufficiently large decrease in the maximum absorbance of MBT in an aqueous medium to indicate the decomposition of the latter under sonocatalytic irradiation. This indicates that the ultrasonic waves which generate the appearance

of reactive radical species such as •OH [64–66] favor the degradation of MBT with an efficiency of 94.29% after 120 min of ultrasonic irradiation.

According to the UV-visible evolution spectrum of the sonocatalytic degradation of MBT by Maghnite-H<sup>+</sup> (Fig. 11) and Table 4, a reaction mechanism could be proposed. Two different paths were considered (Fig. 12): The first step consists of a dehydrogenation reaction with the formulation of MBT-dimer, followed by oxidation by O<sub>2</sub>, which will result in the product BT-SO<sub>2</sub>, which, in turn, is attacked by hydroxyl radicals to give BT-SO<sub>3</sub>H until the opening of the cycles of the molecule and total mineralization (formation: CO<sub>2</sub>, H<sub>2</sub>O, SO<sub>4</sub><sup>(-2)</sup>, ...). The second way corresponds to the loss of the thiol group (-SH), leading to the formation of BT attacked by hydroxyl radicals until total mineralization.

### 3.4 Mineralization efficiency

The mineralization of MBT in both of US/Maghnite-H<sup>+</sup> and US/TiO<sub>2</sub> systems was investigated in terms of TOC removal under certain conditions (pH natural, MBT concentration of 10 mg.L<sup>-1</sup>, Maghnite-H<sup>+</sup> dosage of 3 g.L<sup>-1</sup> and 1.2 g.L<sup>-1</sup> for the TiO<sub>2</sub>-anatase, reaction time of 120 min, frequency of 40 kHz and an ultrasonic power of 120 W). According to the results in Fig. 13, 94.29% MBT removal was obtained during a 120 min, but the degradation of TOC reached to 82.79% after 120 min, this could be related to MBT's oxidation to stable organic molecules and intermediates, which are quantified as TOC [27]. However, only 28.54% TOC was removed even if the reaction time was as long as 120 min, while over 40.22% degradation efficiency was achieved for the US/TiO<sub>2</sub> system. Mineralization generally proceeds significantly more slowly than the degradation of the target compound since degradation is a gradual process, leading first to the formation of organic intermediates and finally to the complete decomposition of the target into CO<sub>2</sub> and inorganic compounds [67].

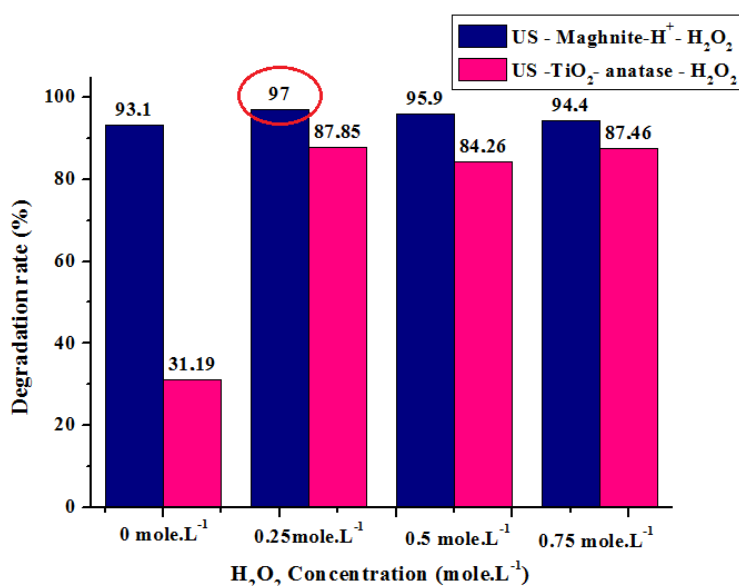


**Figure 10.** Effect of H<sub>2</sub>O<sub>2</sub> concentration on the sonocatalytic degradation of MBT in the presence of Maghnite-H<sup>+</sup> and TiO<sub>2</sub>-anatase. F= 40 kHz, [MBT] =10 mg.L<sup>-1</sup>, [Maghnite-H<sup>+</sup>] = 3 g.L<sup>-1</sup>, [TiO<sub>2</sub>-anatase] = 1.2 g.L<sup>-1</sup>, T = 25 °C.



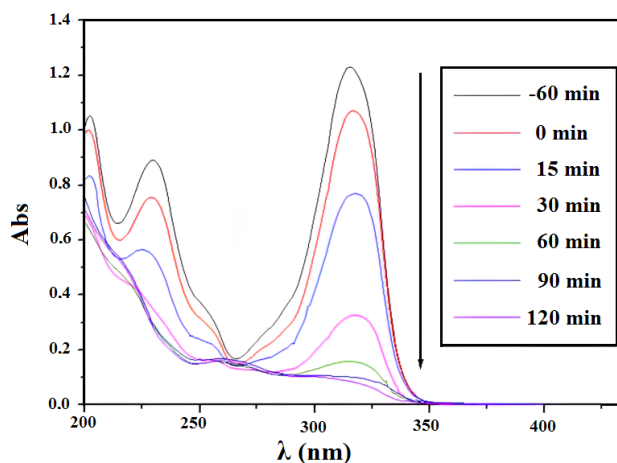


**Figure 11.** UV-Vis absorption spectra of the MBT pollutant for different ultrasonic irradiation times in the presence of Maghnite- $H^+$ .  $F=40\text{ kHz}$ ,  $[Maghnite-H^+]=3\text{ g.L}^{-1}$ ,  $[MBT]=10\text{ mg.L}^{-1}$ ,  $T=25\text{ }^\circ\text{C}$ .

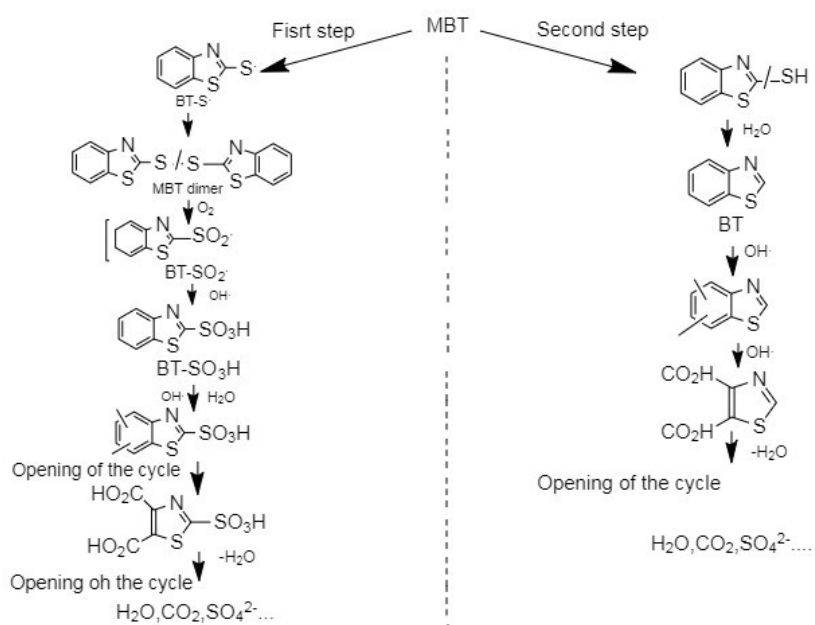


**Figure 12.** Mechanism proposed of MBT degradation in aqueous solution in the presence of Maghnite- $H^+$  under ultrasonic irradiation.

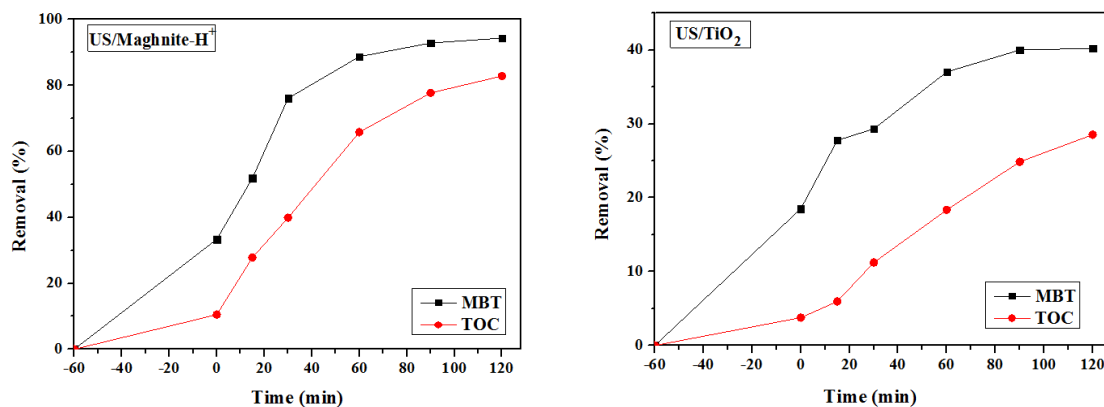


**Figure 13.** Mineralization and degradation of MBT in US/Maghnite- $H^+$  and US/ $TiO_2$  systems.

### 3.5 Comparison with other catalysts

Based on the literature, Table 5 presents a comparative study of different catalysts used in the sonocatalytic degradation process. In this sense, it is possible to confirm, conclusively, that it is possible to obtain a natural source material with catalytic properties and high degradation efficiency using Maghnite-H<sup>+</sup> as a green catalyst.

## 4. Conclusion

In this work, Maghnite-H<sup>+</sup> particles were used as a new green sonocatalyst for the sonocatalytic degradation of 2-Mercaptobenzothiazole (MBT) in an aqueous solution. The results show a better sonocatalytic activity of Maghnite-H<sup>+</sup> compared to that of TiO<sub>2</sub>-anatase via the degradation under ultrasonic irradiation of the organic pollutant MBT. The study carried out showed that the sono-degradation of the latter depends on the dose of the catalyst as well as the initial concentration of MBT. The degradation rate of MBT by Maghnite-H<sup>+</sup> after sonocatalysis for 120 min is 94.29%, and that of TiO<sub>2</sub>-anatase is 40.22%. The addition of H<sub>2</sub>O<sub>2</sub> at a concentration of 0.25 mol.L<sup>-1</sup> shows an improvement in the rate of sonocatalyst degradation due to the production of hydroxyl radicals •OH. The monitoring of the evolution of the absorption spectra of the sonocatalytic degradation of MBT in solution allows two reaction mechanisms of degradation of the MBT molecule to be determined. The TOC removal for MBT in an aqueous solution was achieved at 82.79% and 28.54%, respectively, for US/Maghnite-H<sup>+</sup> and US/TiO<sub>2</sub> systems under the same conditions.

### Acknowledgement

The authors would like to express their sincere thanks to (DGRSDT) the Algerian General Directorate of Scientific Research and Technological Development.

#### Authors Contributions

All authors have contributed equally to prepare the paper.

#### Availability of Data and Materials

The data that support the findings of this study are available from the corresponding author upon reasonable request.

#### Conflict of Interests

The authors declare that they have no known competing financial interests or personal relationships that could have appeared to influence the work reported in this paper.

#### Open Access

This article is licensed under a Creative Commons Attribution 4.0 International License, which permits use, sharing, adaptation, distribution and reproduction in any medium or format, as long as you give appropriate credit to the original author(s) and the source, provide a link to the Creative

Commons license, and indicate if changes were made. The images or other third party material in this article are included in the article's Creative Commons license, unless indicated otherwise in a credit line to the material. If material is not included in the article's Creative Commons license and your intended use is not permitted by statutory regulation or exceeds the permitted use, you will need to obtain permission directly from the OICCPress publisher. To view a copy of this license, visit <https://creativecommons.org/licenses/by/4.0>.

## References

- [1] H. Huang, C. Ma, Z. Zhu, X. Yao, Y. Liu, Z. Liu, C. Li, and Y. Yan. *Chem. Eng. J.*, **338**(2018):218–229. DOI: <https://doi.org/10.1021/cs501631n>.
- [2] S. Bourahla, F. Nemchi, H. Belayachi, A. Belayachi, C. Harrats, and M. Belhakem. *J. Iran. Chem. Soc.*, **20**(2023):669–681, . DOI: <https://doi.org/10.1007/s13738-022-02705-6>.
- [3] L. Li, H. Lin, and S. Qiao. *Light. Sci. Appl.*, **7**(2018): 17138, . DOI: <https://doi.org/10.1038/lsa.2017.138>.
- [4] J. Di, J. Chen, M. Ji, Q. Zhang, L. Xu, J. Xia, and H. Li. *Chem. Eng. J.*, **313**(2017):1477–1485. DOI: <https://doi.org/10.1039/C4TA02400A>.
- [5] J. Li, X. Li, Y. Liu, and J. Zhang. *Chinese J. of Chem. Eng.*, **25**(2)(2010):171–174, . DOI: <https://doi.org/10.1016/j.cjche.2016.08.031>.
- [6] V. Chowanietz, C. Pasel, M. Luckas, T. Eckardt, and D. Bathen. *Ind. Eng. Chem. Res.*, **56**(2017):614–621. DOI: <https://doi.org/10.1021/i260055a023>.
- [7] F.B. Li, X.Z. Li, and K.H. Ng. *Ind. Eng. Chem. Res.*, **45**(2006):1–7, . DOI: <https://doi.org/10.1021/ie050139o>.
- [8] Y. Luo, Z. Lu, Y. Jiang, D. Wang, L. Yang, P. Huo, and P. Yang. *Chem. Eng. J.*, **240**(2014):244–252. DOI: <https://doi.org/10.1016/j.cej.2013.11.088>.
- [9] P. Eghbali, A. Hassani, B. Sündü, and Ö. Metin. *J. Mol. Liq.*, **290**(2019):111208. DOI: <https://doi.org/10.1016/j.molliq.2019.111208>.
- [10] S. Anandan, V. K. Ponnusamy, and M. Ashokkumar. *Ultrason. Sonochem.*, **67**(2020):105130. DOI: <https://doi.org/10.1016/j.ultsonch.2020.105130>.
- [11] A. Hassani, M. Malhotra, A.V. Karim, S. Krishnan, and P.V. Nidheesh. *Environ. Res.*, **205**(2022):112463, . DOI: <https://doi.org/10.1016/j.envres.2021.112463>.
- [12] M.V. Bagal and P.R. Gogate. *Ultrasonics Ultrason. Sonochem.*, **21**(1)(2014):1–14. DOI: <https://doi.org/10.1016/j.ultsonch.2013.07.009>.

- [13] L. Sr, S. Taherian, M.H. Entezari, and N. Ghows. *Ultrason. Sonochem*, **20**(2013):1419–1427. DOI: <https://doi.org/10.1016/j.ultsonch.2013.03.009>.
- [14] N.H. Ince. *Ultrason. Sonochem*, **40**(2018):97–103. DOI: <https://doi.org/10.1016/j.ultsonch.2017.04.009>.
- [15] S. Tangestaninejad, M. Moghadam, and V. Mirkhani. *J. Iran. Chem. Soc.*, **7**(Suppl 2)(2008):S161–S174. DOI: <https://doi.org/10.1007/BF03246195>.
- [16] O. Acisli, A. Khataee, R.D.C. Soltani, and S. Karaca. *Ultrason. Sonochem*, **35**(2017):210–218. DOI: <https://doi.org/10.1016/j.ultsonch.2016.09.020>.
- [17] J.M. Monteagudo, H. El-taliawy, A. Durán, G. Caro, and K. Bester. *J. Hazard. Mater.*, **357**(2018):457–465, . DOI: <https://doi.org/10.1016/j.jhazmat.2018.06.031>.
- [18] F. Liu, P. Yi, X. Wang, H. Gao, and H. Zhang. *Sep. Purif. Technol.*, **194**(2018):181–187. DOI: <https://doi.org/10.1016/j.seppur.2017.10.072>.
- [19] R. Abdelkader and B. Mohammed. *Bull. Chem. React. Eng. Cata*, **11**(2)(2016):170. DOI: <https://doi.org/10.9767/bcrec.11.2.543.170-175>.
- [20] A. Rahmouni. *Bull. Chem. React. Eng. Cata*, **13**(2)(2018). DOI: <https://doi.org/10.9767/bcrec.13.2.1308.262-274>.
- [21] S. Bennabi and M. Belbachir. *J. Inorg. Organom. Polym. Mater.*, (2017):1–13. DOI: <https://doi.org/10.1080/10601325.2017.1339558>.
- [22] H. Khalaf, O. Bouras, and V. Perrichon. *Microporous Mater.*, **8**(1997):141–150. DOI: [https://doi.org/10.1016/S0927-6513\(96\)00079-X](https://doi.org/10.1016/S0927-6513(96)00079-X).
- [23] O. Bouras, M. Houari, and H. Khalaf. *Toxicol. Environ. Chem.*, **70**(1999):221–227. DOI: <https://doi.org/10.1080/02772249909358750>.
- [24] Q. Bao, L. Chen, J. Tian, and J. Wang. *Radiat. Phys. Chem.*, **103**(2014):198–202. DOI: <https://doi.org/10.1016/j.radphyschem.2014.06.001>.
- [25] N. Bensaada, R. Meghabar, and M. Belbachir. *Conférence Matériaux - Colloque Ecomatériau, Montpellier, France*, (2014):hal-01144560f. URL <https://enpc.hal.science/hal-01144560>.
- [26] A. Takdastan, H. Sadeghi, and S. Dobaradaran. *J. Iran. Chem. Soc.*, **17**(2020):725–734. DOI: <https://doi.org/10.1007/s13738-019-01809-w>.
- [27] N. Jaafarzadeh, A. Takdastan, S. Jorfi, F. Ghanbari, M. Ahmadi, and G. Barzegar. *J. Mol. Liq.*, **256**(2018):462–470. DOI: <https://doi.org/10.1016/j.molliq.2018.02.047>.
- [28] S. Jin, L. Hong-fu, W. Qing-Ping, X. Zheng-Miao, and C. Zu-liang. *Desalination*, **280**(2011):167–173. DOI: <https://doi.org/10.1016/j.desal.2010.10.056>.
- [29] H. Zaghouane-Boudiaf, M. Boutahala, S. Sahnoun, C. Tiar, and F. Gomri. *Appl. Clay Sci.*, **90**(2014):81–87. DOI: <https://doi.org/10.1016/j.clay.2013.12.030>.
- [30] D. Garmia, H. Zaghouane-Boudiaf, and C.V. Ibbora. *Int. J. Biol. Macromol.*, **115**(2018):257–265. DOI: <https://doi.org/10.1016/j.ijbiomac.2018.04.064>.
- [31] Z. Li, B. Hou, Y. Xu, D. Wu, and Y. Sun. *J. Colloid Interface Sci.*, **288**(2005):149–154, . DOI: <https://doi.org/10.1016/j.jcis.2005.02.082>.
- [32] S. Bourahla, C. Harrats, H. Belayachi, F. Nemchi, and M. Belhakem. *Desalin. Water Treat.*, **104**(2018):324–329, . DOI: <https://doi.org/10.5004/dwt.2018.21905>.
- [33] C.H. Zhou, S. Xu, Y. Yang, B.C. Yang, H. Hu, Z.C. Quan, B. Sebo, B.L. Chen, Q.D. Tai, Z.H. Sun, and X.Z. Zhao. *Electrochim. Acta.*, **56**(2011):4308–4314, . DOI: <https://doi.org/10.1016/j.electacta.2011.01.054>.
- [34] A. Harrane, R. Meghabar, and M. Belbachir. *Int. J. Mol. Sci.*, **3**(2002):790–800, . DOI: <https://doi.org/10.3390/i3070790>.
- [35] A. Harrane and M. Belbachir. *Macromol. Symp.*, **247**(1)(2007):379–384. DOI: <https://doi.org/10.1002/masy.200750144>.
- [36] E. Aslyya, A. Harrane, and M. Belbachir. *Mater. Res.*, **19**(2016):132–137. DOI: <https://doi.org/10.1590/1980-5373-MR-2015-0322>.
- [37] M. Ghadiri, W. Chrzanowski, and R. Rohanizadeh. *RSC Adv.*, **5**(2015):29467–29481. DOI: <https://doi.org/10.1039/C4RA16945J>.
- [38] W. Shuo, D. Zhu, C. Xue, X. Jun, and W. Dan-Hong. *Catalysts*, **10**(7)(2020):759. DOI: <https://doi.org/10.3390/catal10070759>.
- [39] A. Harrane, R. Meghabar, and M. Belbachir. *Des. Monomers Polym.*, **8**(1)(2005):11–24, . DOI: <https://doi.org/10.1163/1568555053084203>.
- [40] D.E. Kherroub, M. Belbachir, and S. Lamouri. *Green Process. Synth.*, **7**(4)(2018):296–305, . DOI: <https://doi.org/10.1515/gps-2017-0033>.
- [41] D.E. Kherroub, M. Belbachir, and S. Lamouri. *Res. Chem. Intermed.*, **43**(10)(2017):5841–5856, . DOI: <https://doi.org/10.1007/s11164-017-2966-8>.
- [42] L. Palliyaguru, U.S. Kulathunga, and L.I. Jayarathna. *Int. J. Miner. Metall. Mater.*, **27**(2020):846–855. DOI: <https://doi.org/10.1007/s12613-020-2030-3>.
- [43] R.G. Toro, M. Diab, T. De Caro, M. Al-Shemy, A. Adel, and D. Caschera. *Materials*, **13**(6)(2020):1326. DOI: <https://doi.org/10.3390/ma13061326>.
- [44] S.A. Hamdan, I.M. Ibrahim, , and I.M. Ali. *Dig. J. Nanomater. Bios.*, **15**(4)(2020):1001–1008. DOI: <https://doi.org/10.15251/DJNB.2020.154.1001>.

- [45] V.B. Mohan, K. Jayaraman, and D. Bhattacharyya. *Sol. State Commun*, **320**(2020):114004. DOI: <https://doi.org/10.1016/j.ssc.2020.114004>.
- [46] F. Macht, K. Eusterhues, G.J. Pronk, and K.U. Totsche. *Appl. Clay. Sci*, **53**(2011):20–26. DOI: <https://doi.org/10.1016/j.clay.2011.04.006>.
- [47] M. Ayat, M. Belbachir, and A. Rahmouni. *Polym. Bull*, **75**(2018):5355–5371. DOI: <https://doi.org/10.1007/s00289-018-2328-8>.
- [48] Y. Bouznit, Y. Beggah, A. Boukerika, and F. Lahreche. *Appl. Surf. Sci*, **284**(2013):936–941. DOI: <https://doi.org/10.1016/j.apsusc.2013.03.155>.
- [49] R. Mehdaoui, L. Chaabane, and E. Beyou. *J. Iran. Chem. Soc*, **16**(2019):645–659. DOI: <https://doi.org/10.1007/s13738-018-1539-0>.
- [50] Y. Zhang and X. Xu. *ACS Publications*, **5**(25)(2020):15344–15352. DOI: <https://doi.org/10.1021/acsomega.0c01438>.
- [51] A. Allaoui, M.A. Malouki, and P. Wong-Wah-Chung. *J. Photochem. Photobiol*, **A212**(2010):153–160. DOI: <https://doi.org/10.1016/j.jphotochem.2010.04.010>.
- [52] L.L. He, X.P. Liu, Y.X. Wang, Z.X. Wang, Y.J. Yang, Y.P. Gao, B. Liu, and X. Wang. *Ultrason. Sonochem*, **33**(2016):90–98. DOI: <https://doi.org/10.1016/j.ultsonch.2016.04.028>.
- [53] M. Karaca, M. Kiransan, S. Karaca, A. Khataee, and A. Karimi. *Ultrason. Sonochem*, **31**(2016):250–256. DOI: <https://doi.org/10.1016/j.ultsonch.2016.01.009>.
- [54] L. Song, S. Zhang, X. Wu, and Q. Wei. *Ultrason. Sonochem*, **19**(6)(2012):1169–1173. DOI: <https://doi.org/10.1016/j.ultsonch.2012.03.011>.
- [55] A. Hassani, P. Eghbali, and O. Metin. *Environ. Sci. Pollut. Res*, **25**(32)(2018):32140–32155. DOI: <https://doi.org/10.1007/s11356-018-3151-3>.
- [56] A. Khataee, P. Eghbali, M.H. Irani-Nezhad, and A. Hassani. *Ultrason. Sonochem*, **48**(2018):329–339. DOI: <https://doi.org/10.1016/j.ultsonch.2018.06.003>.
- [57] M. Zhou, H. Yang, T. Xian, R.S. Li, H.M. Zhang, and X.X. Wang. *J. Hazard. Mater*, **289**(2015):149–157. DOI: <https://doi.org/10.1016/j.jhazmat.2015.02.054>.
- [58] I. Fatimah, R. Nurillahi, I. Sahroni, G. Fadillah, B.H. Nugroho, A. Kamari, and O. Muraza. *J. Water Process. Eng*, **37**(2020):101418. DOI: <https://doi.org/10.1016/j.jwpe.2020.101418>.
- [59] M. Chauhan, N. Kaur, P. Bansal, R. Kumar, S. Srinivasan, and G.R. Chaudhary. *J. Nanomater*, **vol. 2020**(2020):15. DOI: <https://doi.org/10.1155/2020/6123178>.
- [60] L. Xu, X. Wang, M.L. Xu, B. Liu, X.F. Wang, S.H. Wang, and T. Sun. *Ultrason. Sonochem*, **61**(2020):104815. DOI: <https://doi.org/10.1016/j.ultsonch.2019.104815>.
- [61] A. Touati, L. Jlaiel, W. Najjar, and S. Sayadi. *Euro-Mediterr. J. Environ. Integr*, **4**(2019):4. DOI: <https://doi.org/10.1007/s41207-018-0086-5>.
- [62] F. Siadatnasab, S. Farhadi, and A. Khataee. *Ultrason. Sonochem*, **44**(2018):359–367. DOI: <https://doi.org/10.1016/j.ultsonch.2018.02.051>.
- [63] F. Siadatnasab, S. Farhadi, M. Dusek, V. Eigner, A.A. Hoseini, and A. Khataee. *Ultrason. Sonochem*, **64**(2020):104727. DOI: <https://doi.org/10.1016/j.ultsonch.2019.104727>.
- [64] S. Chong, G. Zhang, Z. Wei, N. Zhang, T. Huang, and Y. Liu. *Ultrason. Sonochem*, **34**(2017):418–425. DOI: <https://doi.org/10.1016/j.ultsonch.2016.06.023>.
- [65] A.J. Ruíz-Baltazar. *Ultrason. Sonochem*, **73**(2021):105521. DOI: <https://doi.org/10.1016/j.ultsonch.2021.105521>.
- [66] J.M. Monteagudo, H. El-taliawy, A. Durán, G. Caro, and K. Bester. *J. Hazard. Mater*, **357**(2018):457–465. DOI: <https://doi.org/10.1016/j.jhazmat.2018.06.031>.
- [67] M. Magureanu, N. Bogdan Mandache, and Vasile I. Parvulescu. *Water Res*, **81**(2015):124–136. DOI: <https://doi.org/10.1016/j.watres.2015.05.037>.